Index

North Sea FLOW Measurement Workshop

Paper 6.1

Pressure and Temperature Effects for Ormen Lange Ultrasonic Gas Flow Meters – Results from a Follow-Up Study

Per Lunde
University of Bergen

Kjell-Eivind Frøysa
Christian Michelsen Research AS (CMR)

Vincent Martinez and Øyvind Torvanger
CMR Prototech

TÜV SÜD

nel technology for life

26th International North Sea Flow Measurement Workshop
21st – 24th October 2008

Pressure and Temperature Effects for Ormen Lange Ultrasonic Gas Flow Meters - Results from a Follow-up Study

Per Lunde, University of Bergen
Kjell-Eivind Frøysa, Christian Michelsen Research AS (CMR)
Vincent Martinez, CMR Prototech
Øyvind Torvanger, CMR Prototech

ABSTRACT

Ultrasonic gas flow meters may be influenced by pressure and temperature in several ways. Change of the meter body's cross-sectional area (the "pipe bore") influences directly on the amount of gas flowing through the meter. Change of the ultrasonic path geometry (i.e. change of the inclination angles and lateral chord positions, caused by e.g. spoolpiece diameter change and change of the orientation of the ultrasonic transducer ports) influences on the transit times and the numerical integration method of the meter. Change of the Reynolds number influences on the integration method. Change of the length of the ultrasonic transducer ports influences on the acoustic path lengths, and thus on the transit times. Likewise, change of the length of the ultrasonic transducers influences on the acoustic path lengths, and thus on the transit times. In addition, changes of the transducer properties such as the directivity, influences on the diffraction correction, and thus on the transit times.

Some of these issues are addressed to some extent in current draft standards for such meters, such as the AGA-9 (1998) report, and the ISO/CD 17089-1 (2007). Other of these effects have not been described or treated in the literature.

In 2007, a paper was given at the NSFMW'07 [2] on pressure and temperature effects for five 18" Instromet Q-Sonic 5 ultrasonic flow meters (USMs) operated in the Ormen Lange fiscal metering system at Nyhamna in Møre and Romsdal, Norway, from October 2007. Pressure and temperature changes from flow calibration (Westerbork, at 63 barg and 7 ^{o}C) to field operation (Ormen Lange, nominally at 230 barg and 40 ^{o}C) conditions were evaluated. The effects addressed were changes related to (A) the meter's cross-sectional area, (B) the ultrasonic path geometry (inclination angles and lateral chord positions), (C) length expansion of the ultrasonic transducer ports, (D) length expansion/compression of the ultrasonic transducers, and (E) Reynolds number correction.

The various effects (A)-(E) contributing to the measurement error were discussed and quantified. Investigations were made using a combination of analytical modeling and finite element numerical modeling (FEM) of the meter body and the ultrasonic transducers, combined with a model for USM numerical integration relevant for the Q-Sonic 5 multipath ultrasonic flow meter in question.

Two correction factors were proposed for the Q-Sonic 5 in this application: (1) one "nominal P&T correction factor" (accounting for by far the largest part of the correction, about 0.26 %), and (2) an "instantaneous P&T correction factor" (accounting for small deviations in pressure and temperature from nominal to actual Ormen Lange conditions), which is typically an order of magnitude smaller than the nominal P&T correction factor. The correction factors and the individual contributors to these were discussed and quantified.

There has been raised some questions (cf. e.g. [3]) in relation to the results presented in [1,2], and on basis of such discussions, a follow-up study has been initiated.

In the present paper, pressure effects on the meter body related to the effects (A) and (B) have been revisited and analysed in more detail, for three different "meter body geometries", cylindrical pipe, flanged pipe, and flanged pipe with ultrasonic transducer ports (the Ormen Lange Q-Sonic 5 meter body). These cases have been analyzed with respect to influence of axial boundary conditions ("ends free", "ends clamped", "ends capped"), and influence of the

meter body wall thicknesses. A combination of finite element modelling (FEM) and analytical modelling has been used for this purpose.

It has been found that with respect to pressure effects on the inner radius displacement, the cylindrical pipe thick-shell model (cf. "Roark formuls") with either "ends free" or "ends capped" axial boundary conditions provides a good approximation for all three "meter body geometries" considered here, for wall thicknesses up to $w/R_0 = 0.25$. The corresponding thin-shell models (cf. "Roark formulas") represent relatively poor approximations in the range $w/R_0 = 0.05 - 0.25$.

The results show that for the Ormen Lange project, the actual axial boundary condition being used ("ends free", "ends clamped" or "ends capped") is not critical for calculation of the radial displacement and the pressure correction factor. That is, the boundary conditions approach taken in [1,2], where the "ends free" boundary condition was used, should be a valid and relatively accurate approach. For the Ormen Lange meter, the uncertainty of the volumetric flow rate measurement due to the choice of axial boundary condition made in the calculation of the "nominal P&T correction factor", is estimated to about ±0.01 %.

1 INTRODUCTION

From October 2007 five 18" Elster-Instromet Q-Sonic ultrasonic gas flow meters (USMs) have been operated at a land based fiscal gas metering station at Nyhamna, Møre and Romsdal, Norway, for export of gas through the 1200 km Langeled pipeline, to an import metering station in Easington, UK, built by Statoil, cf. Fig.1. The Ormen Lange export station at Nyhamna was constructed and built by Norsk Hydro, and is now operated by Shell. The production life of Ormen Lange is estimated to 50 years.

The nominal flow rate of the Ormen Lange export metering station is 70 million Sm^3/day, or 25 billion Sm^3/year. At an assumed sales price of 2 NOK/Sm^3 this corresponds tentatively to 140 million NOK/day, or 50 billion NOK/year. An assumed systematic measurement error of only 0.3 % (as an example), would correspond to about 420 000 NOK/day, or about 153 million NOK/year, for such a tentative sales price.

Flow calibration of the flow meters have been made at the Westerbork laboratory in the Netherlands, at temperature and pressure conditions of 7 °C og 63 barg, respectively, with two meters in series installed in a "long pipe", and with flow conditioner upstream of the meters.

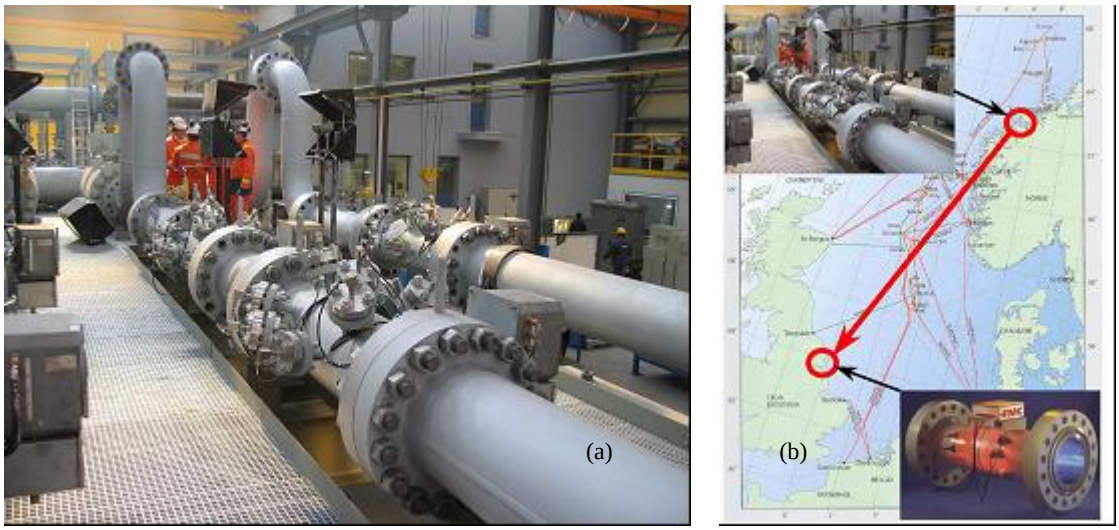

Fig. 1. *(a) Photograph of the Ormen Lange fiscal gas metering station, under factory acceptance test (FAT) in Athens, Greece, 2005. (After [1,2].)*
(b) Sketch of the Ormen Lange transport system, with fiscal metering stations at Nyhamna (Norway) and Easington (UK). (After [1,2].)

The high pressures in question at the Ormen Lange metering station, 230 barg nominal, have raised the question whether correction for pressure and temperature effects on the USMs will be needed, relative to the 63 barg pressure used under flow calibration at Westerbork.

Pressure and temperature effects on the ultrasonic meters relates to factors such as e.g.

(A) Change of the meter's cross-sectional area,
(B) Change of the ultrasonic path geometry (inclination angles and lateral chord positions),
(C) Change of the length of the ultrasonic transducer ports,
(D) Change of the length of the ultrasonic transducers,
(E) Change of the Reynolds number,
(F) Diffraction correction effects.

In [1,2], the various effects (A)-(E) contributing to the measurement error have been analyzed and quantified. Investigations were made using a combination of analytical modeling and finite element numerical modeling of the meter body and the ultrasonic transducers, combined with a model for USM numerical integration relevant for the Q-Sonic 5 multipath ultrasonic flow meter in question.

In [1,2], two correction factors were proposed for the Q-Sonic 5 in this application:

(1) a "nominal P&T correction factor" (accounting for by far the largest part of the correction, about 0.26 %), and
(2) an "instantaneous P&T correction factor" (accounting for small deviations in pressure and temperature from nominal to actual Ormen Lange conditions), which is typically an order of magnitude smaller than the nominal P&T correction factor.

The correction factors and the individual contributors to these were discussed and quantified. It was concluded that for the Ormen Lange application, evaluation of all of the factors (A)-(E) are necessary to establish the effect of pressure and temperature on the meter. Finite element modeling (FEM) calculations indicated that the combined effect of (A) change of the meter's cross-sectional area (diameter change) and (B) change of the ultrasonic path geometry (inclination angles and lateral chord positions) are by far the largest and most dominant effects, amounting to about 0.246 %. Of this number, the pressure and temperature effects were found to be responsible for 0.121 % and 0.125 %, respectively. The total effect of (A) – (E) was calculated to be 0.262 % (the "nominal P&T correction factor").

There has been raised some questions (cf. e.g. [3]) in relation to the results presented in [1,2], and on basis of such discussions, a follow-up (Phase 2) study has been initiated by Shell on behalf of the Ormen Lange partners, on an initiative from the Norwegian Petroleum Directorate (NPD). The follow up-study is carried out by Christian Michelsen Research AS (CMR) in cooperation with the University of Bergen, Norway.

In the present paper, selected and central topics from this follow-up study are addressed. The analysis and discussion is here limited to the effects (A) and (B) in the list above, since these are by far the dominating sources of measurement error in the Ormen Lange application [1,2]. Moreover, the present analysis is limited to pressure effects, since there has been no remarks in relation to the way temperature effects are treated in [1,2]. The temperature correction was made in agreement with ISO/CD 17089-1 recommendations [6].

The topics addressed here in relation to pressure effects on (A) and (B) are:

- For the FEM analysis on which the "nominal P&T correction factor" was based in [1,2], "ends free" boundary conditions were used at the meter body ends. Boundary conditions play a major role in the outcome of any FEM exercise, and - since the approach used in [1,2] may be questioned [3] - a number of scenarios are run here to investigate the sensitivity of the results to different boundary conditions. Four different axial boundary conditions are investigated: (a) "ends free", (b) "ends clamped", (c) "ends capped (bolt circle curve load)" and (d) "ends capped (flange surface load)" (cf. Section 3.1).

- For the comparably small and significantly less important "instantaneous P&T correction factor", a thin-wall pipe theory was used in [1,2]. Thus, this thin-wall theory was used only for very small pressure changes (a few bars). However, it has been commented [3] that since the actual meter body is clearly a thick-wall vessel (the thickness/radius ratio of the body is 0.25 while the indicated "thin-wall limit" is 0.1 [5]), the estimation of the deflection using thin-wall theory may be questioned. Comparison of thin- and thick-wall theories with FEM results are thus made here, to investigate the need for using thick-wall theory for the relatively small pressure effects in the "instantaneous P&T correction factor".

The objective of the present paper is thus - through a more refined and extended FEM analysis of pressure effects on the meter body - to get improved insight into the validity and accuracy of the analysis and results presented in [1,2].

2 SPECIFICATIONS

The specifications for the study are the same as in [1,2], repeated here for convenience and completeness.

The Ormen Lange metering station consists of 3 parallel meter runs, with in total 5 ultrasonic flow meters, cf. Fig. 1:

- 2 parallel runs, each with two 18" ultrasonic flow meters in series,
- 1 parallel run with one 18" ultrasonic flow meter, for backup measurement,
- Flow conditioner will be used (DN450 Laws type 316SS or Duplex Material),
- Elster-Instromet Q-Sonic 5 ultrasonic gas flow meters [4].

Table 1 gives various parameters of the USM, and Table 2 other specifications for the study. For other details on the Q-Sonic 5 meter of relevance for the study, it is referred to [1,2].

With respect to the topic under study here, it is noted that the pressure change from Westerbork (flow calibration) to nominal Ormen Lange (operating) conditions is ΔP_{mc} = (230 – 63) bar = 167 bar, cf. Table 2.

Table 1. Specifications of the ultrasonic flow meters used in the Ormen Lange metering station.

Parameter	Property	Conditions
Material type	Steel (Duplex)	
Length, L_0	1800 mm	(at assumed 20 °C, 1 atm.)
Outer diameter, *OD*	457.2 mm	(at assumed 20 °C, 1 atm.)
Inner diameter, *ID*	(366.5 ± 0.25) mm	(at assumed 20 °C, 1 atm.)
Inner radius, R_0	183.25 mm	(at assumed 20 °C, 1 atm.)
Wall thickness, *w*	45.35 mm	(at assumed 20 °C, 1 atm.)
w/R_0	0.25	(at assumed 20 °C, 1 atm.)
Young's modulus, *Y*	$2.0 \cdot 10^5$ MPa	
Poisson's ratio, σ	0.3	
Coeff. of linear thermal expansion, α	$12.6 \cdot 10^{-6}$ K^{-1} (ASME)	

Table 2. Specifications for the study.

Parameter	Westerbork flow calibration conditions	Ormen Lange metering station (line conditions, nominal)
Gas	Dry natural gas	Dried natural gas[a)]
Pressurel *P*	63 barg	230 barg (design)
Temperature	7 °C	40 °C (design)
Viscosity	$1.30 \cdot 10^{-5}$ Pa-s	$2.28 \cdot 10^{-5}$ Pa-s
Density	57.36 kg/m^3	186.6 kg/m^3
Metering configuration	2 USMs in series, with upstream flow conditioner	2 USMs in series, with upstream flow conditioner
Flow velocity	1.5 – 19 m/s	Volumetric flow rate 70 MSm^3/d (=> flow velocity = 15-16 m/s per run)
Reynolds number, *Re*	$2.4 \cdot 10^6$ – $3.0 \cdot 10^7$	$4.5 \cdot 10^7$

[a)] The gas composition is known, but has not been necessary to specify for the present study.

3 ANALYSIS METHODS

The analysis methods used in the study are described in the following.

3.1 Boundary Conditions (Axial Constraints)

The deformations of the meter body are quite dependent on how the pipe is constrained. To investigate the sensitivity of the results to different boundary conditions, three different cases of axial constraint are studied: (a) "ends free", (b) "ends clamped", and (c) "ends capped".

”Ends free” boundary conditions imply that the spool is free to deform axially, and that the interior pressure does not induce any axial loads. An example of this case is a pressurized pipe where at least one of the ends is resting on an o-ring or another dynamic seal. In a straight pipe the pressure will only cause tangential tensile stresses. The pipe will contract in the axial direction due to the Poisson effect.

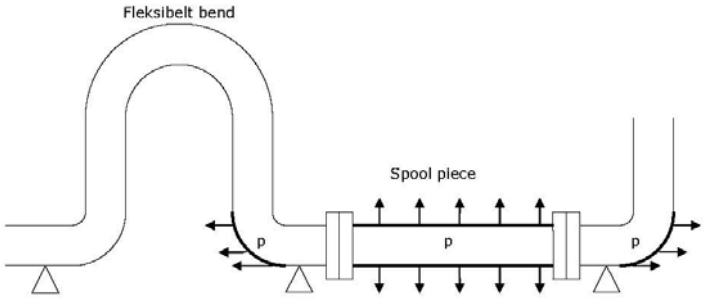

Fig. 2. Sketch of pipeline section in which the meter is mounted, illustrating the loads on a meter body (spoolpiece) due to pressure. The pipe is free to slide on the supports.

”Ends clamped” boundary conditions imply that the spool is fixed against axial movement (no axial displacement at the two end surfaces of the pipe). An example of this case is a long straight rock dumped pipe. This pipe is not able to deform axially. The pressure will cause tangential tensile stresses, but also axial tensile stresses due to the Poisson effect. If this pipe is heated, the thermal expansion may cause axial compressive stresses, causing buckling if the rock dump is insufficient.

”Ends capped” boundary conditions imply that the spool is free to deform axially, and that the pressure also induces axial loads. An example of this case is a capped (closed) pipe (a pressure tank). An other example of this case is a pipe resting on sliding supports, connected to a flexible bend (cf. Fig. 2). The pressure will cause both tangential tensile stresses and axial tensile stresses. The axial stresses are caused by a pressure against an end cap or a bend, and are transferred through the bolts of the flanges. This is a common design of piping to avoid compressive stresses in the piping and to avoid large loads in the foundations. However, even in a flexible bend there will be some stiffness, causing axial stresses in the spool.

3.2 Simulation series overview

Table 3 gives an overview of the simulation series described in the present paper. Three different "meter body geometries" are considered: (a) a cylindrical (straight) pipe, (b) a flanged pipe, and (c) a flanged pipe with transducer ports (equal to the Ormen Lange Q-Sonic 5 meter body). All have the same length L_0 and inner radius R_0 at "dry calibration" conditions (20 ^{o}C, 1 atm., cf. Table 2), and the wall thickness / inner radius ratio w/R_0 is varied in five steps from 0.05 to 0.25, where the latter value relates to the Ormen Lange case.

In this study, each of these "meter body geometries" are subjected to different axial constraints, as described in Section 3.1: (a) "ends free", (b) "ends capped", and (c) "ends clamped". For all of these cases, finite element calculations (FEM) are made (cf. Section 3.4). In addition, analytical (simplified) theory is used whenever available (cf. Section 3.3).

Table 3. Meter body geometries, axial boundary conditions, and calculation analysis methods used in the present study.

Meter body geometry	Axial boundary conditions	Type of analysis
Cylindrical pipe 	Ends free	• Thin shell theory (Roark) • Thick shell theory (Roark) • FEM
	Ends capped (tank)	• Thin shell theory (Roark) • Thick shell theory (Roark) • FEM
	Ends clamped	• FEM
Flanged pipe 	Ends free	• FEM
	Ends capped (tank)	• FEM
	Ends clamped	• FEM
Flanged pipe, w/ transducer ports 	Ends free	• FEM
	Ends capped (tank)	• FEM
	Ends clamped	• FEM
"Flanged-in meter body" (ISO 17089-1, 2007)	-	• Thin shell theory
"Welded-in meter body" (ISO 17089-1, 2007)	-	• Thin shell theory

3.3 Analytical calculation models

In ultrasonic transit time flow meters with reflecting and/or non-reflecting paths, the volumetric flow rate (at line conditions) is given as [6-8][1]

$$q_{USM} = \pi R^2 \sum_{i=1}^{N} w_i (N_{refl,i} + 1) \frac{2\sqrt{R^2 - y_i^2}\,(t_{1i} - t_{2i})}{t_{1i} t_{2i} \left|\sin 2\phi_i\right|} \,. \tag{1}$$

"Analytical model A". At a temperature T_m and pressure P_m, the meter body radius (R), the lateral chord positions (y_i), and the inclination angles (ϕ_i), can be shown to be approximately given by [8,1,2]

$$R \approx K_T K_P R_c \,, \qquad y_i \approx K_T K_P y_{ic} \,, \qquad \phi_i \approx \tan^{-1}\left(\frac{\tan(\phi_{ic})}{1 - (1 - \beta^*/\beta)(K_P - 1)} \right), \qquad i = 1, \ldots, N \tag{2}$$

where subscript "*c*" is used to denote the respective geometrical quantity at flow calibration (Westerbork) conditions, i.e. R_c, y_{ic} and ϕ_{ic}. The correction factors for the inner radius of the meter body due to dimensional changes caused by temperature and pressure changes relative to flow calibration conditions, are given as (cf. e.g. [9-12])

$$K_T \equiv 1 + \alpha \Delta T_{mc} \,, \qquad \Delta T_{mc} \equiv T_m - T_c \,, \tag{3}$$

$$K_P \equiv 1 + \beta \Delta P_{mc} \,, \qquad \Delta P_{mc} \equiv P_m - P_c \,, \tag{4}$$

respectively. Eqs. (2)-(4) are referred to as the "analytical model A" [1,2], and applies to all inclination angles.

[1] Symbols are defined at the end of the paper.

"Analytical model B". For USMs where all inclination angles are equal to ±45°, q_{USM} can - from Eqs. (1)-(4) - be written as [8,1]

$$q_{USM} \approx q_{USM,c} \cdot C_{tsm} \cdot C_{psm} \quad , \tag{5}$$

where

$$C_{tsm} = K_T^3 = (1+\alpha\Delta T_{mc})^3 \approx 1+3\alpha\Delta T_{mc} \, , \quad C_{psm} = K_P^3 = (1+\beta\Delta P_{mc})^3 \approx 1+3\beta\Delta P_{mc} \, . \tag{6}$$

Eqs. (5)-(6) are referred to as the "analytical model B" [1,2]. The main advantage of the analytical model B over model A lays in the fact that in model B, the *P* and *T* corrections of the geometrical quantities of the meter body can be separated from the basic USM functional relationship and put outside of the summing over paths, as illustrated by Eq. (5). For USMs with inclination angles equal to ±45°, the analytical model B is equivalent to the analytical model A. For other inclination angles it represents an approximation to the more accurate analytical model A [8]. This is the case for Q-Sonic 5, which employ inclination angles of 60° and 70°.

Table 4. Thin and thick cylindrical shell models, for different axial boundary conditions, taken from ref. [5] (Roark formulas), Table 13.1 (p. 592, cases 1b and 1c) and Table 13.5 (p. 683, cases 1a and 1b). (Blank fields: analytical theory not identified.)

Axial boundary conditions	Type of theory	$\frac{\Delta R}{R_0}$	$\frac{\Delta L}{L_0}$	β	β'
Ends free	Thin shell	$\frac{\Delta R}{R_0} = \frac{R_0}{wY}\Delta P$	$\frac{\Delta L}{L_0} = -\frac{R_0\sigma}{wY}\Delta P$	$\beta = \frac{R_0}{wY}$	$\beta' = -\frac{R_0\sigma}{wY}$
	Thick shell	$\frac{\Delta R}{R_0} = \frac{1}{Y}\left(\frac{(R_0+w)^2+R_0^2}{(R_0+w)^2-R_0^2}+\sigma\right)\Delta P$	$\frac{\Delta L}{L_0} = -\frac{\sigma}{Y}\frac{2R_0^2}{(R_0+w)^2-R_0^2}\Delta P$	$\beta = \frac{1}{Y}\left(\frac{(R_0+w)^2+R_0^2}{(R_0+w)^2-R_0^2}+\sigma\right)$	$\beta' = -\frac{\sigma}{Y}\frac{2R_0^2}{(R_0+w)^2-R_0^2}$
Ends clamped	Thin shell		0		0
	Thick shell		0		0
Ends capped	Thin shell	$\frac{\Delta R}{R_0} = \frac{R_0}{wY}\left(1-\frac{\sigma}{2}\right)\Delta P$	$\frac{\Delta L}{L_0} = \frac{R_0}{wY}(0.5-\sigma)\Delta P$	$\beta = \frac{R_0}{wY}\left(1-\frac{\sigma}{2}\right)$	$\beta' = \frac{R_0}{wY}(0.5-\sigma)$
	Thick shell	$\frac{\Delta R}{R_0} = \frac{1}{Y}\left(\frac{(R_0+w)^2(1+\sigma)+R_0^2(1-2\sigma)}{(R_0+w)^2-R_0^2}\right)\Delta P$	$\frac{\Delta L}{L_0} = \frac{1}{Y}\frac{R_0^2(1-2\sigma)}{(R_0+w)^2-R_0^2}\Delta P$	$\beta = \frac{1}{Y}\left(\frac{(R_0+w)^2(1+\sigma)+R_0^2(1-2\sigma)}{(R_0+w)^2-R_0^2}\right)$	$\beta' = \frac{1}{Y}\frac{R_0^2(1-2\sigma)}{(R_0+w)^2-R_0^2}$

Coefficients of linear pressure expansion. The radial and axial linear pressure expansion coefficients β and β* involved in the analytical models A and B depend on the type of support provided for the meter body installation (i.e. the boundary conditions). For cylindrical and isotropic elastic meter bodys, analytical models for β and β* taken from the "Roark formulas" [5] are given in Table 4. For reference and to enable comparison, the two analytical models used in ISO/CD 17089-1 [6] are also included here, cf. Table 5.

Table 5. Thin shell models, for different pipe geometry / mounting conditions, taken from ref. [6] (ISO/CD 17089-1). (Blank fields: analytical theory not available.)

Mounting conditions	Type of theory	$\frac{\Delta R}{R_0}$	$\frac{\Delta L}{L_0}$	β	β'
Flanged-in meter body	Thin shell	$\frac{\Delta R}{R_0} = 0.5\frac{R_0}{wY}\Delta P$		$\beta = 0.5\frac{R_0}{wY}$	
Welded-in meter body	Thin shell	$\frac{\Delta R}{R_0} = 1.17\frac{R_0}{wY}\Delta P$		$\beta = 1.17\frac{R_0}{wY}$	

3.4 Finite element modelling (FEM)

The analytical models A and B described in Section 3.3 represent simplified descriptions, accounting for "average" effects, and may in general not be able to account very precisely for the effects of pressure on the meter body. To analyze such effects in more detail and more accurately (including effects of flange thickness, wall thickness, the resulting form of the meter body (e.g. pipe bulging), influence of the transducer ports and their location, displacement of the transducer ports, precise calculation of the ultrasonic path lengths, etc.), a numerical finite element model (FEM) is needed.

Thus, as a second and considerably more accurate step to analyze pressure effects on the Q-Sonic 5 ultrasonic meter body, a FEM approach has been used. The finite element meshes used for FEM calculations of the three "meter body geometries" considered here are shown in Fig. 3. Dimensional changes caused by pressure changes, at any position of the meter body, may be calculated using FEM.

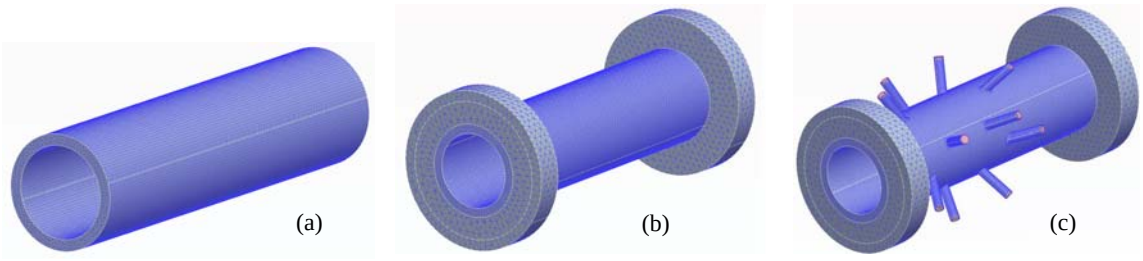

Fig. 3. Finite element mesh used for FEM analysis of P effects for (a) a cylindrical pipe, (b) a flanged pipe, and (c) flanged pipe with transducer ports (the Ormen Lange Q-Sonic 5 meter body).

For the calculations shown here, the NASTRAN (Version 2007.0.0 Release 1) finite element program is used, with the tetrahedral solid element CTETRA [7]. The end of the transducer ports are modelled using the shell elements CQUAD4 and CTRIA3, to enable extraction of the rotations at the transducer port extremities. The material data used for the calculations are given in Table 1.

The mesh control features used are the following:

- Maximum allowed element size: 40 mm for the flanges, 14 mm for the pipe, 4 mm for the transducer ports,
- Minimum forced element size: 20 mm for the flanges, 10 mm for the pipe, 2 mm for the transducer ports,
- Hard points with defined node identification (transducer port ends, and axial profile lines).

Three load cases are used, “ends free”, “ends clamped” and “ends capped”, cf. Section 3.1.

For the two cases “ends free” and “ends capped” the model is constrained against rigid body motion in all 6 degrees of freedom. The model is held in space, but it is free to deform under stress.

For the “ends clamped” case the model is also constrained against rigid body motion in all 6 degrees of freedom, but the flange end surfaces are additionally fully constrained against axial deformation. For the “ends capped” case, two different methods of applying the axial load are used: “bolt circle curve load” and “flange surface load”.

For the flanged pipe, an additional sub-load case is defined under the “ends free” and “ends capped” constraints, where the flanges are constrained against orthoaxial rotation. Rigid bars are used for this purpose, forcing the flange surfaces to be parallel. It has been found that the “no rotation” constraint has only a local influence on the deformed profile. The critical profile area where the transducers are located (in the mid section of the body), does not vary significantly whether the “no rotation” constraint is used or not [11] (not shown here).

The FEM calculations give in principle the change of position for every point of the meter body. Thus, the change of diameter in the horizontal and vertical directions and changes with respect to the transducer ports (i.e. inclination angles and directional orientation of the port (rotation, etc.)), are calculated. This includes the rotation around the vertical, axial and transversal axes, of the back plane of the transducer ports [14].

4 RESULTS AND DISCUSSION

The simulation results of the study are given in the present section. Finite element (FEM) calculations are shown in subsections 4.1 and 4.2, for a cylindrical pipe, a flanged pipe, and a flanged pipe with transducer ports (the full Q-Sonic 5 meter body). The wall thickness / inner radius ratio is w/R_0 = 0.25, and the pressure difference is ΔP_{mc} = (230 – 63) bar = 167 bar. Comparisons of the FEM results with the analytical calculation models described in subsection 3.3 are given in subsection 4.3.

4.1 Cylindrical (Straight) Pipe, and Flanged Pipe

FEM calculations for the cylindrical pipe are given in Fig. 4a, for 3 different boundary conditions: "ends free", "ends clamped" and "ends capped". The calculated radial displacement is relatively uniform along the pipe, ranging from about 74 µm, 70 µm to 66 µm, for the 3 types of boundary conditions, respectively.

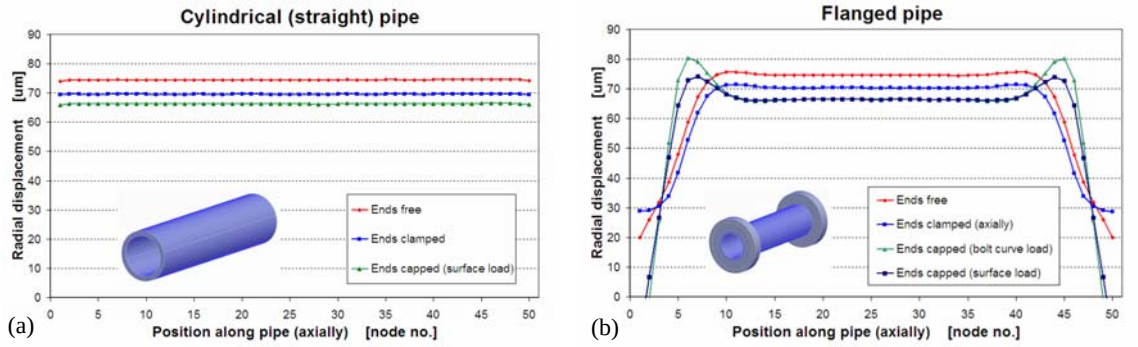

Fig. 4. Inner radius displacement of (a) a cylindrical pipe and (b) a flanged pipe, for ΔP_C = 167 bar and wall thickness / radius ratio w/R_0 = 0.25, calculated using finite element modelling (FEM).

Corresponding FEM calculations for the flanged pipe are given in Fig. 4b, for 4 different boundary conditions: "ends free", "ends clamped", "ends capped (bolt circle curve load)", and "ends capped (flange surface load)". The flanged pipe has the same dimensions as the Q-Sonic 5 meter body, and differs from the real meter body only by the absence of transducer ports. In all cases the radial displacement is highly non-uniform along the pipe, due to the flanges. This is also illustrated in Fig. 5. Of significant importance for the present study is the distribution of the radial displacement along the pipe. In the mid section of the pipe, outside the flange region (between nodes 10 and 40), the calculated radial displacement is relatively uniform along the pipe, ranging from about 75 µm, 70 µm to 67 and 67 µm, for the 4 types of boundary conditions, respectively. This is important, as this is the region in which the transducer ports and the acoustic paths are located.

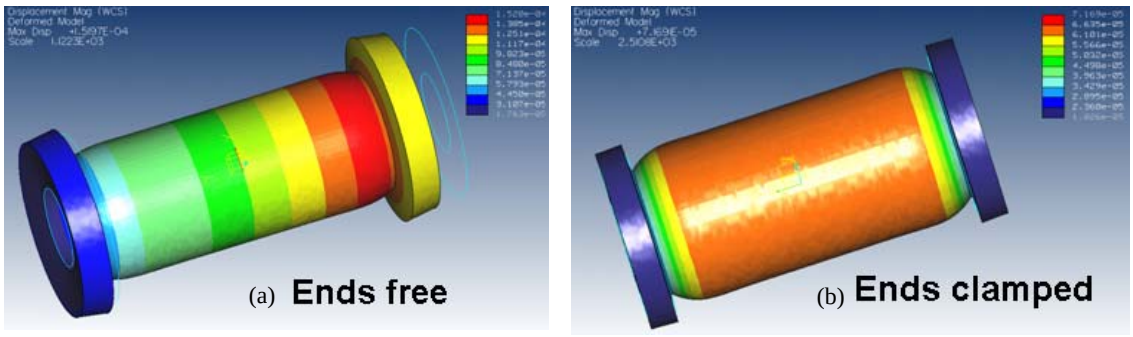

Fig. 5. FEM calculation of the pressure expansion of a flanged pipe with the same dimensions as the Ormen Lange Q-Sonic 5 meter body, for ΔP_{mc} = 167 bar and w/R_0 = 0.25. Boundary condition: (a) "ends free" and (b) "ends clamped"..

4.2 Flanged Pipe With Transducer Ports (Q-Sonic 5 Meter Body)

An example of a FEM calculation for the flanged pipe with transducer ports (the Ormen Lange Q-Sonic 5 meter body) is shown in Fig. 6, for the case of "ends free" boundary conditions. Due to the presence of the transducer ports, the radial displacement shows some asymmetry around the meter body, and to achieve representative quantitative figures for the radial displacement over the body, the radial displacement is calculated along four axial profile lines along the inner wall, denoted Line 1 (12 o'clock = 0°), Line 2 (9 o'clock = 270°), Line 3 (6 o'clock = 180°) and Line 4 (3 o'clock = 90°). FEM calculation results along these four lines are shown in Fig. 7, for 4 different boundary conditions: "ends free", "ends clamped", "ends capped (bolt circle curve load)", and "ends capped (flange surface load)".

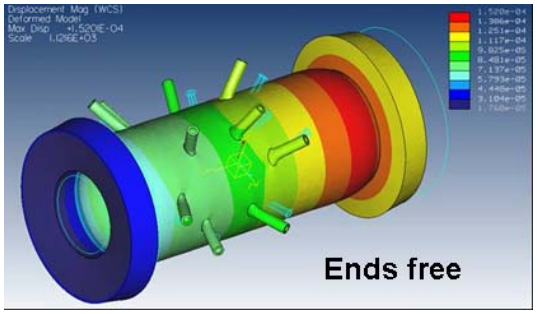

Fig. 6. FEM calculation of the pressure expansion of the Ormen Lange Q-Sonic 5 meter body, for ΔP = 167 bar and w/R = 0.25. Boundary condition: "ends free".

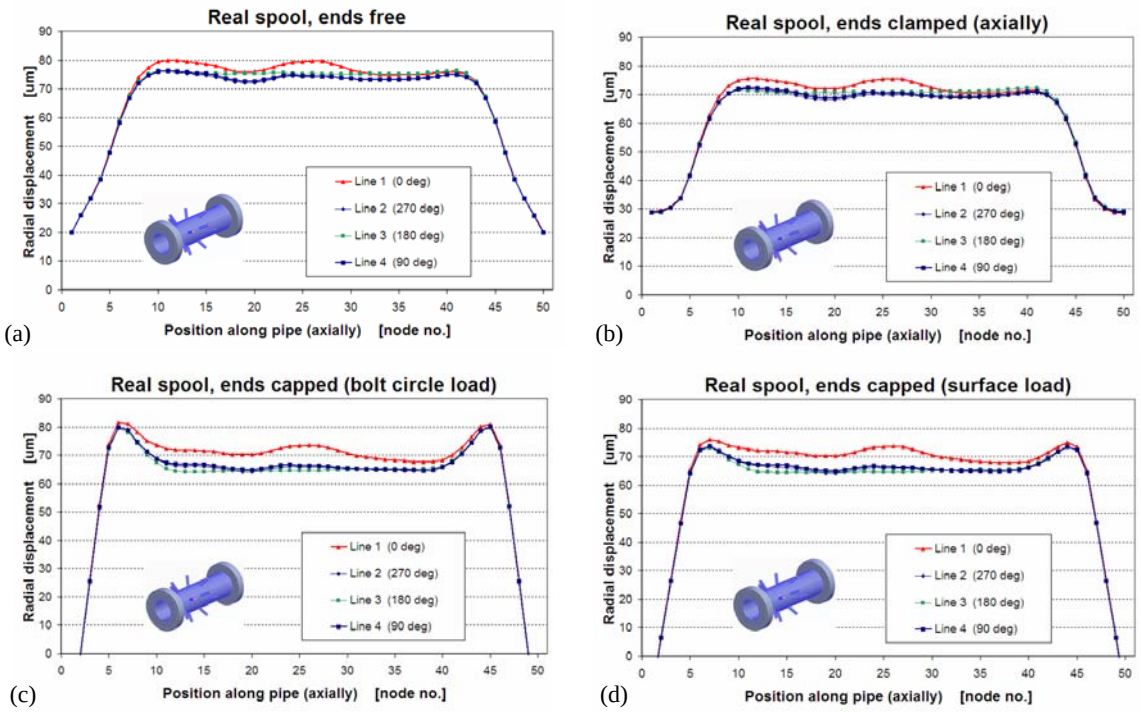

Fig. 7. Inner radius displacement of the Q-Sonic 5 meter body (with w/R_0 = 0.25) for ΔP_{mc} = 167 bar and different boundary conditions: (a) "ends free", (b) "ends clamped", (c) "ends capped (bolt circle curve load)" and (d) "ends capped (flange surface load)", calculated using FEM.

It is noted from Fig. 7 that the radial displacement is highly non-uniform along the pipe, similar to the flanged pipe in Fig. 4b. In the mid section of the pipe, outside the flange region (between nodes 10 and 40), the calculated radial displacement is relatively uniform along the pipe, but not as uniform as for the flanged pipe. This variation along the pipe is due to the presence of the transducer ports. The transducer ports are also responsible for the asymmetry observed around the pipe center axis. In the mid section of the pipe (between nodes 10 and 40), the calculated radial displacement ranges from about 64 μm to 80 μm, for the 4 profile lines and the 4 types of boundary conditions.

4.3 Comparison Of Results, With Discussion

The results shown in Sections 4.1 and 4.2 have been calculated for a wall thickness / inner radius ratio equal to w/R_0 = 0.25, as for the Ormen Lange Q-Sonic 5 meter body. Similar calculations have been made also for the ratios w/R_0 = 0.05, 0.10, 0.15 and 0.20, to (a) investigate the influence of wall thickness, w, on the behaviour of the meter body, (b) for comparison with analytical thin- and thick-wall theories, and (c) to establish a more general and representative data set as a basis for the conclusions of the study. All calculations have been made for a pressure change ΔP_{mc} = (230 – 63) bar = 167 bar (cf. Table 2).

It should be noted that in order to limit the simulation series and the number of parameters to be accounted for in the study, the flange thickness has been kept constant over the simulation series (that is, constant for all w/R_0), equal to the flange thickness of the full Ormen Lange Q-Sonic 5 meter body with w/R_0 = 0.25 [1,2]. In reality, a reduced wall thickness would of course be accompanied by a reduced flange thickness. However, the results obtained in the study, with a relatively wide "flat" mid section (cf. Figs. 4-7, and similar results for lower w/R_0, not shown here), indicate that this potential limitation does not seem to be a significant and important limitation of the study, and of minor importance for the conclusions.

Figs. 8, 9 and 10 show the inner radius displacement as a function of w/R_0, for the different calculation models (analytical and FEM) and "meter body geometries" (cylindrical pipe, flanged pipe, Q-Sonic-5 meter body), for different axial boundary conditions, "ends free", "ends clamped" and "ends capped", respectively. Parts (a) of the figures show the calculated inner radius displacement (ΔR) in mm, while parts (b) of Figs. 8 and 10 show the ratio of the calculated relative inner radius displacement ($\Delta R/R_0$) to the respective relative inner radius displacement of the thin-wall theory $(\Delta R/R_0)_{thinshell}$ (for the axial boundary condition in question). Only the absolute and relative radial changes, ΔR and $\Delta R/R_0$, are considered here[2].

Besides of the FEM calculations of the different meter body geometries, Figs. 8 and 10 also show calculations using the analytical thin-wall and thick-wall "Roark formulas" given in Table 4, for "ends free" and "ends capped" boundary conditions, respectively.

With respect to the FEM calculations of the different meter body geometries, the figures shown have been calculated as follows. For the cylindrical pipe, the radial displacement (as in Fig. 4a for w/R_0 = 0.25) has been averaged over the complete pipe length. For the flanged pipe, the radial displacement (as in Fig. 4b for w/R_0 = 0.25) has been averaged over the mid section of the pipe (nodes 10 to 40), since that is the region in which the transducer ports (and thus the acoustic paths) are located. (The regions close to the flanges are not of interest in that respect.) For the Q-Sonic 5 meter body (marked "flanged pipe, transd ports" in Figs. 8-10) the figures shown are calculated as follows. Firstly, for each axial profile line 1-4, the average displacement is calculated over the mid section of the line (nodes 10 to 40), for the same reason as for the flanged pipe (cf. Fig. 5 for w/R_0 = 0.25). Secondly, these average displacements for the 4 lines are averaged, to achieve a single number which represents the average radial displacement for the mid section of the Q-Sonic 5 meter body.

[2] The absolute and relative length changes, ΔL and $\Delta L/L_0$, have also been calculated (using the two analytical "Roark formulas" of Table 4 as well as FEM calculations for the three different "meter body geometries") (cf. [14]), but these results are not shown here.

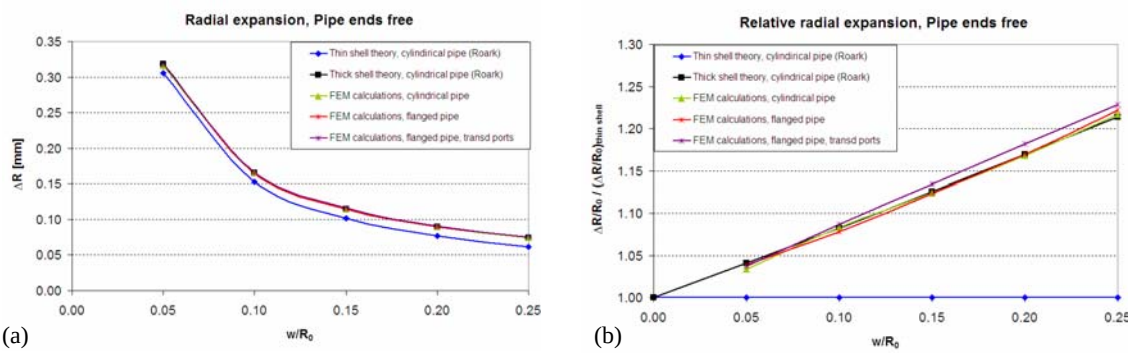

Fig. 8. Comparison of inner radius displacement obtained using different calculation models (the 2 cylindrical pipe models of Table 4 ("Roark formulas"), and 3 FEM calculations), for "ends free" boundary conditions, for ΔP_{mc} = 167 bar. (a) Inner radius displacement, and (b) inner radius displacement relative to the thin-shell theory (with "ends free" boundary conditions).

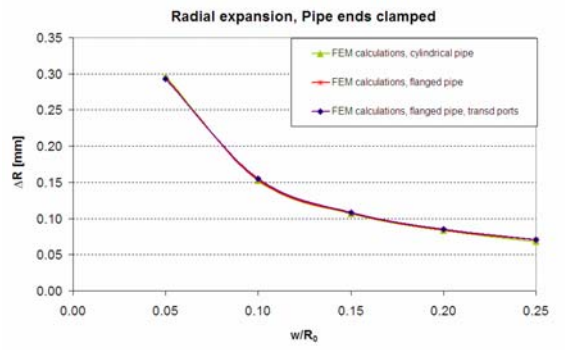

Fig. 9. Comparison of inner radius displacement (inner radius displacement) obtained using different calculation models (3 FEM), for "ends clamped" boundary conditions, for ΔP_{mc} = 167 bar. (Note that analytical models have not been available for this boundary condtion, cf. Table 4.)

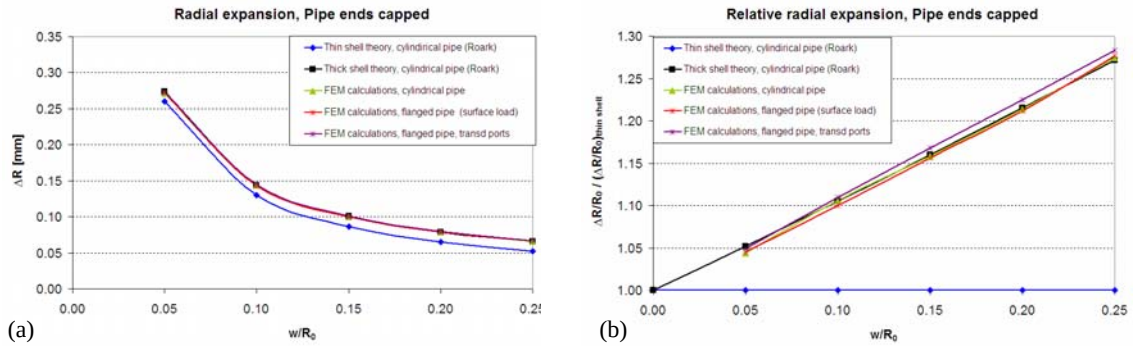

Fig. 10. Comparison of inner radius displacement obtained using different calculation models (the 2 cylindrical pipe models of Table 4 ("Roark formulas"), for "ends capped" boundary conditions, for ΔP_{mc} = 167 bar. (a) Inner radius displacement, and (b) inner radius displacement relative to the thin-shell theory (with "ends capped" boundary conditions).

First, consider parts (a) of Figs. 8-10, giving the absolute radial displacement (ΔR) in mm. It is noted that for the two types of axial boundary conditions for which analytical theories have been available, "ends free" and "ends capped" pipe constraints, the thin-shell models predict too low radial displacement, over the complete range of w/R_0 investigated, 0.05 to 0.25. From part (b) of Figs. 8 and 10, it follows that for w/R_0 = 0.1, the underestimation of the thin-shell models is about 8 and 10 % for the two boundary conditions, respectively, whereas for w/R_0 = 0.25, the underestimation is about 22 and 27 %, respectively.

The thick-shell models, however, are found to be in relatively close agreement with the FEM calculations for the cylindrical pipe. Moreover, the thick-shell models are in relatively close agreement also with the FEM calculations for the flanged pipe, and in fair agreement with the FEM calculations for the flanged pipe with transducer ports (the Q-Sonic 5 type of meter body). It appears that the radial displacement is slightly larger for the flanged pipe with transducer ports than for the cylindrical and flanged pipes, especially for large w/R_0. This is

ascribed to a reduced effective stiffness of the body wall due to the holes in wall caused by the transducer ports.

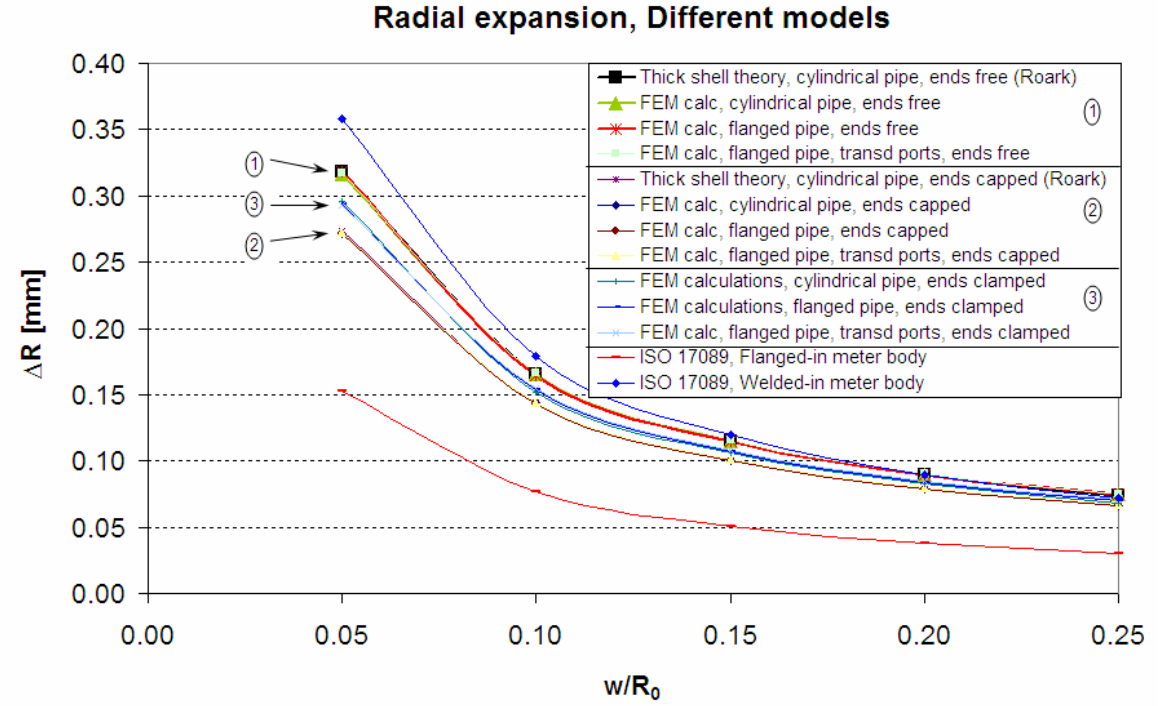

Fig. 11. Comparison of the radial displacement results shown in Figs. 7a, 8 and 9a (thin-shell model results excluded), with the 2 models used in ISO/CD 17089-1 (cf. Table 5).

From the above results, three important questions arise. Firstly, to what extent do the radial displacement results depend on the various boundary conditions? Secondly, how do these results compare with the results predicted by the ISO/CD 17089-1 models given in Table 5? And thirdly, what are the consequences for the volumetric flow rate measured by the USM?

Fig. 11 shows a comparison of the results given in of Figs. 8-10 (with the thin-shell model results excluded), together with the results predicted by the two ISO/CD 17089-1 models given in Table 5. It appears that the results are falling in five "groups", where the first three are indicated in the figure. Group nos. 1-3 contain the results for the "ends free", "ends capped" and "ends clamped" boundary conditions, respectively. Within each of these groups, there is a close agreement between the various calculations, as discussed above. For lower w/R_0, the three groups differ somewhat, whereas for w/R_0 approaching 0.25 the difference between the three groups becomes relatively small.

The other two "groups" in Fig. 11 are the ISO/CD 17089-1 model results. The "flanged-in meter body" model severely underestimates the radial displacement, whereas the "welded-in meter body" model gives results which at lower w/R_0 are higher than the other models, but becomes in agreement with groups 1–3 as w/R_0 approaches 0.25.

Fig. 12 shows the volumetric pressure correction factor, C_{psm}, calculated using the simplified model given by Eqs. (5)-(6), which is strictly valid only for USM inclination angles equal to 45^o. We find the same type of "grouping" and model behaviour as described above for the radial displacement isolated, in Fig. 11. It should be noted, however, that C_{psm} accounts for effects of both (A) the radial displacement (the change of cross-sectional area) and (B) the change of ultrasonic path geometry (due to the movement of the transducer ports), as discussed in Section 3.3.

From Eq. (5), the (percentage) influence of these two factors (A) and (B) on the volumetric flow rate measurement, Q, is given as $(C_{psm}\text{-}1)*100\%$ (still according to the simplified model, however, with inclination angles equal to 45^o). These types of result are shown in Fig. 13, for the various calculation models and "meter body geometries" discussed in the present paper.

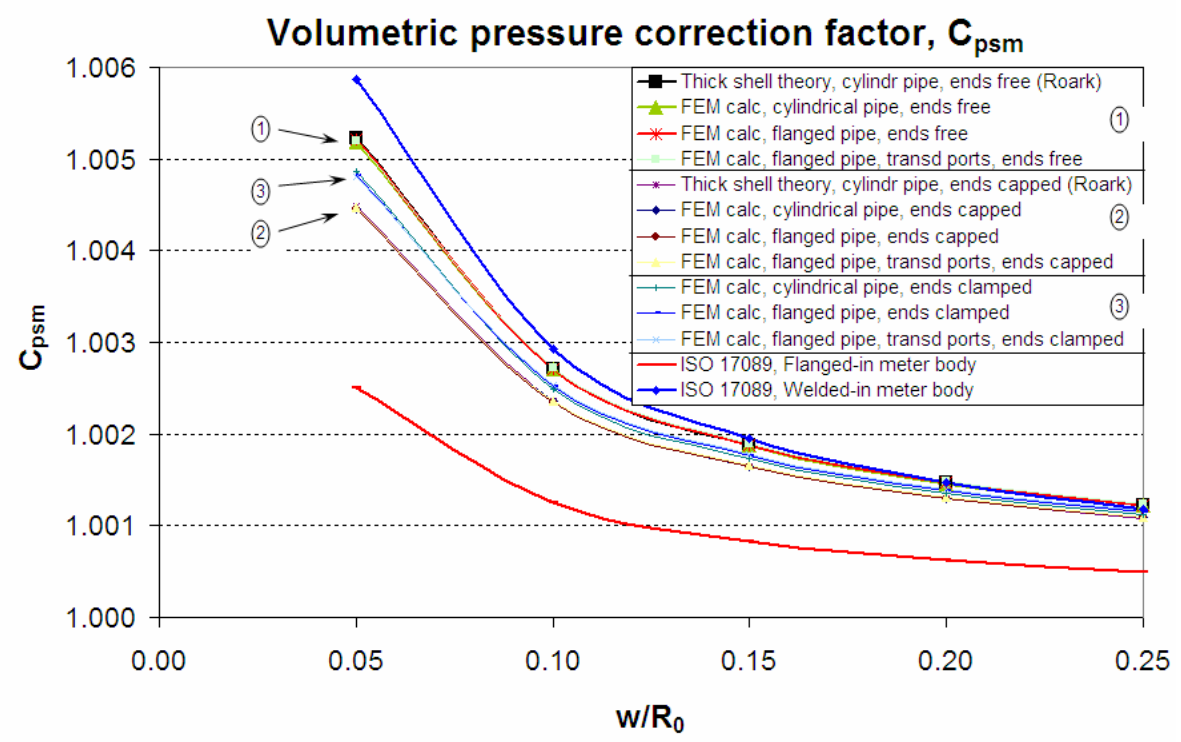

Fig. 12. Volumetric pressure correction factor, C_{psm}, for the Q-Sonic 5 meter body, calculated using different models, as a function of wall thickness – inner radius ratio.

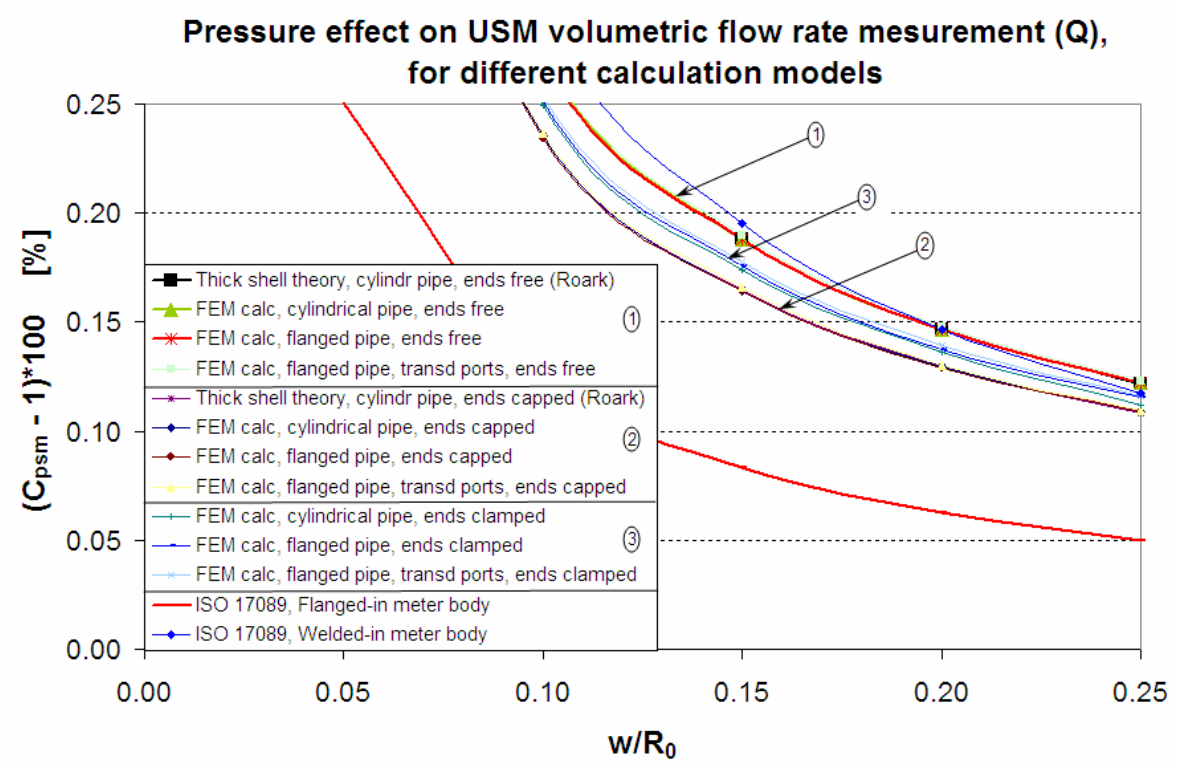

Fig. 13. Pressure effect on USM volumetric flow rate measurement (Q) for the Q-Sonic 5 meter body, calculated using different models, as a function of wall thickness – inner radius ratio.

Again, the results fall into five groups, where the first three are indicated in the figure, for the "ends free", "ends capped" and "ends clamped" boundary conditions, respectively. Within each of these groups, there is also here a good agreement between the various calculations.

For w/R_0 approaching 0.25 the difference between the three groups becomes relatively small, but not negligible. For the Ormen Lange meter, with w/R_0 = 0.25, the pressure effect is calculate to be about (0.12 ± 0.01) %, where the indicated "uncertainty" accounts for the deviation between groups 1-3 only. That is, if an "uncertainty" of 0.01 % is acceptable for the Ormen Lange project, the actual axial boundary condition being used ("ends free", "ends capped" and "ends clamped") should not be critical for calculation of the radial displacement and the pressure correction factor.

Fig. 13 also shows the ISO/CD 17089-1 model results. The "flanged-in meter body" model provides a severe underestimation, and is not recommended. The "welded-in meter body" model, on the other hand, gives results which for w/R_0 approaching 0.25, becomes in agreement with the groups 1–3.

However, on background of the general pattern apparent in the above results, both of the thick-shell models given in Table 4 ("Roark formulas", for "ends free" and "ends capped" boundary conditions) seem to provide more representative results than the "welded-in meter body" model given in Table 5. This is so for cylindrical pipes, flanged pipes as well as for flanged pipes with transducer ports (the Q-Sonic 5 meter body), and for all three types of axial boundary conditions considered, "ends free", "ends capped" and "ends clamped". The Roark thick shell models also have the advantage that they are derived mathematically from physical principles, and account for both radial and length changes of the pipe.

5 SUMMARY AND CONCLUSIONS

In [1,2] (for Phase 1 of the study) correction factors were proposed for P & T effects on the 18" Q-Sonic 5 ultrasonic flow meters, from Westerbork flow calibration conditions (63 barg and 7 °C) to Ormen Lange line conditions (nominally at 230 barg and 40 °C). The proposed correction factors account for several P & T effects, such as

(A) Change of the meter's cross-sectional area,
(B) Change of the ultrasonic path geometry (inclination angles and lateral chord positions),
(C) Change of the length of the ultrasonic transducer ports,
(D) Change of the length of the ultrasonic transducers,
(E) Change of the Reynolds number.

For the Ormen Lange application, it was shown in [1,2] that evaluation of all of the effects (A) – (E) have been necessary to evaluate the effect of pressure and temperature on the meter.

In the present paper, under Phase 2 of the study, pressure effects on the meter body related to the effects (A) and (B) have been revisited and analysed in more detail, for three different "meter body geometries",

- cylindrical (straight) pipe,
- flanged pipe,
- flanged pipe with ultrasonic transducer ports (the Ormen Lange Q-Sonic 5 meter body),

with respect to

- influence of axial boundary conditions ("ends free", "ends clamped", "ends capped"), and
- influence of meter body wall thickness.

A combination of finite element modelling (FEM) and analytical modelling has been used for this purpose. Meter body wall thicknesses in the range w/R_0 = 0.05 - 0.25 have been studied.

It has been found that with respect to pressure effects on the inner radius displacement, the cylindrical pipe thick-shell model with either "ends free" or "ends capped" axial boundary conditions (cf. the "Roark formulas", cf. Table 4) provides a good approximation for all three "meter body geometries" considered here (cylindrical pipe, flanged pipe, and flanged pipe with ultrasonic transducer ports), for wall thicknesses up to w/R_0 = 0.25.

The thin-shell models (cf. the "Roark formulas", cf. Table 4) represent relatively poor approximations in the range w/R_0 = 0.05 - 0.25. Since the complexities in implementation of the thick- and thin-shell models are similar, the thick-shell model should in general be preferred, due to its significantly higher accuracy.

It may thus be preferable to use one of the thick shell models for calculation of the "instantaneous P&T correction factor" for the Ormen Lange meter. Since this factor is to account for the small excess gas pressure relative to the nominal pressure of 230 barg only (i.e. a few bars), the results using the Roark thin- and thick shell models may not deviate much. However, by using the more accurate thick shell model, discussions in relation to this point may be avoided.

The results are compared with two models used in ISO/CD 17089-1, the "flanged-in meter body" and the "welded-in meter body" models [6], cf. Table 5. The "flanged-in meter body" model provides a severe underestimation, and is not recommended. The reason for the underestimation using this model is expected to be the fact that the mid section of the USM (in which the transducer ports and the acoustic paths are located) expands relatively uniformly with pressure, which possibly violates the pressure expansion assumption underlying the "flanged-in meter body" model.

The "welded-in meter body" model [6] yields results which for w/R_0 close to 0.25 are in close agreement with the results using the Roark thick-shell and FE models. However, in general the results demonstrate that the two thick-shell models (the "Roark formulas", cf. Table 4) provide more representative results than the "welded-in meter body" model. This is so for cylindrical pipes, flanged pipes as well as for flanged pipes with transducer ports (including the Q-Sonic 5 meter body), and for all three types of axial boundary conditions considered, "ends free", "ends capped" and "ends clamped". Both of the thick-shell models may thus be preferred as compared with the "welded-in meter body" model, for all cases mentioned above.

It has been shown here that for the Ormen Lange project, the actual axial boundary condition being used ("ends free", "ends clamped" or "ends capped") is not critical for calculation of the radial displacement and the pressure correction factor. That is, the boundary conditions approach taken in [1,2], where the "ends free" boundary condition was used, should be a valid and relatively accurate approach. For the Ormen Lange meter, the uncertainty of the volumetric flow rate measurement due to the choice of axial boundary condition made in the calculation of the "nominal P&T correction factor", is estimated to about $\pm$0.01 %.

The implications of the results reported here with respect to the "nominal P&T correction factor" and the "instantaneous P&T correction factor" proposed in [1,2], will be documented and reported in an unclassified technical report, to be available early 2009, at the completion of the ongoing Phase 2 of the project [14].

SYMBOL NOTATION

P_0 : gas pressure at "dry calibration" conditions (taken to be 1 atm. = 101325 Pa)
P_c : gas pressure at flow calibration (Westerbork) conditions [Pa]
P_m : gas pressure at operating (Ormen Lange) conditons [Pa]
ΔP_{mc} : change of gas pressure from flow calibration (Westerbork) to operating (Ormen Lange) conditons [m]
T_0 : gas temperature at "dry calibration" conditions (taken to be 20 ^oC)
T_c : gas temperature at flow calibration (Westerbork) conditions [^oC]
T_m : gas temperature at operating (Ormen Lange) conditons [^oC]
ΔT_{mc} : change of gas temperature from flow calibration (Westerbork) to operating (Ormen Lange) conditons [m]
R_0 : inner radius of USM meter body at "dry calibration" conditions (taken as 1 atm. and 20 ^oC) [m]
R_c : inner radius of USM meter body, at flow calibration (Westerbork) conditions [m]

R : inner radius of USM meter body, at operating (Ormen Lange) conditions [m]

ΔR : change of inner radius of USM meter body, from flow calibration (Westerbork) to operating (Ormen Lange) conditons = $R - R_c$ [m]

L_0 : length of USM meter body, at "dry calibration" conditions (taken as 1 atm. and 20 ^oC) [m]

ΔL : change of length of USM meter body, from flow calibration (Westerbork) to operating (Ormen Lange) conditons [m]

w : wall thickness of USM meter body, at "dry calibration" conditions (taken to be 1 atm. and 20 ^oC) [m]

Y : Young's modulus for the meter body material [Pa]

σ : Poisson's ratio for the meter body material [-]

α : coefficient of linear thermal expansion of the meter body material [K^{-1}]

β : radial linear pressure expansion coefficient of the meter body [Pa^{-1}]

β^* : axial (length) linear pressure expansion coefficient of the meter body [Pa^{-1}]

K_T : radial temperature correction factor for the USM meter body [-]

K_P : radial pressure correction factor for the USM meter body [-]

C_{tsm} : volumetric temperature correction factor for the USM meter body [-]

C_{psm} : volumetric pressure correction factor for the USM meter body [-]

q : corrected volumetric flow rate at line (Ormen Lange) conditions [m^3/s]

q_{USM} : volumetric flow rate output from the USM at line (Ormen Lange) conditions [m^3/s]

$q_{USM,c}$: volumetric flow rate output from the USM at flow calibration (Westerbork) conditions [m^3/s]

N : number of acoustic paths in the USM [-]

w_i : integration weight factor for acoustic path no. i of the USM [-]

L_i : interrogation length for path no. i, at operating (Ormen Lange) conditions [m]

y_i : lateral distance from the pipe center (lateral chord position) for path no. i, at operating (Ormen Lange) conditions [m]

ϕ_i : inclination angle (relative to the pipe axis) of path no. i, at operating (Ormen Lange) conditions [radians]

y_{ic} : lateral distance from the pipe center (lateral chord position) for path no. i, at flow calibration (Westerbork) conditions [m]

ϕ_{ic} : inclination angle (relative to the pipe axis) of path no. i, at flow calibration (Westerbork) conditions [radians]

t_{1i} , t_{2i} : measured transit times for upstream and downstream sound propagation of path no. i [s]

$N_{refl,i}$: number of wall reflections for path no. i ($N_{refl,i}$ = 0, 1 or 2 in current USMs), i = 1, …, N [-]

ACKNOWLEDGEMENTS

The authors wish to thank the Ormen Lange partners for the possibility to publish the present paper. Comments given in discussions with the Ormen Lange project (in particular StatoilHydro and Shell representatives) and the Norwegian Petroleum Directorate (NPD) have been of great value to the study.

REFERENCES

[1] **P. Lunde, and K.-E. Frøysa**, "Ormen Lange ultrasonic gas flow meters. A study for establishment of corrections for pressure and temperature effects", CMR report no. CMR-06-A10048-RA-01, Christian Michelsen Research AS, Norway (March 2007).

[2] **P. Lunde, K.-E. Frøysa and T. Folkestad**, "Pressure and temperature effects for Ormen Lange ultrasonic gas flow meters", Proc. of *25th International North Sea Flow Measurement Workshop, Oslo, Norway, 16-19 October 2007.*

[3] **R.J. Whitson**, "Review of report: "Ormen Lange ultrasonic gas flow meters. A study for establishment of corrections for pressure and temperature effects"", Report no. 2007/290, TUV-NEL Ltd., Glasgow, Scotland (December 2007).

[4] Elster-Instromet Q-Sonic 5 ultrasonic flow meter web site, Elster-Instromet NV, Rijkmakerlaan 9, B-2910 Essen, Belgium (2006); http://www.elster-instromet.com/en/ultrasonic_flow_metering.html

[5] **W. C. Young and W. C. Budynas**, *Roark's formulas for stress and strain*, 7th edition (McGraw-Hill, New York, 2001).

[6] **"**Measurement of flow in closed conduits – ultrasonic meters for gas – Part 1: meters for custody transfer and allocation measurement", ISO/CD 17089-1, August 31, 2007, International Organization for Standardization, Genéve, Switzerland. (Committee Draft.) (Reference number ISO/TC 30/SC 05 N210.)

[7] "GERG project on ultrasonic gas flow meters, Phase II", edited by Lunde, P., Frøysa, K.-E. and Vestrheim, M., GERG TM11 2000, Groupe Européen de Recherches Gazières (VDI Verlag, Düsseldorf, 2000).

[8] **Lunde, P. and Frøysa, K.-E.:** "Handbook of uncertainty calculations. Ultrasonic fiscal gas metering stations". Handbook prepared on behalf of the Norwegian Society of Oil and Gas Measurement (NFOGM) and the Norwegian Petroleum Directorate (NPD) (December 2001), 279 p. (ISBN 82-566-1009-3). (Free download available from www.nfogm.no.)

[9] "Manual of petroleum measurement standards. Chapter 12 - Calculation of petroleum quantities. Section 2 - Calculation of liquid petroleum quantites measured by turbine or displacement meters", First edition. American Petroleum Institute, U.S.A. (September 1981). (Paragraphs 12.2.5.1 and 12.2.5.2.)

[10] "Manual of petroleum measurement standards. Chapter 12 - Calculation of petroleum quantities. Section 2 - Calculation of liquid petroleum quantites using dynamic measurement methods and volumetric correction factors. Part 1 - Introduction", Second edition. American Petroleum Institute, Washington D.C., U.S.A. (May 1995). (Paragraphs 1.11.2.1 and 1.11.2.2.)

[11] **"**Institute of Petroleum. Petroleum Measurement Manual. Part X - Meter Proving. Section 3 - Code of practice for the design, installation and calibration of pipe provers", Published on behalf of The Institute of Petroleum, London (J. Wiley & Sons, Chichester, 1989), Section 10.7, p. 31 (ISBN 0 471 92231 5).

[12] "Measurement of gas by ultrasonic meters", A.G.A. Report no. 9, American Gas Association, Transmission Measurement Committee (June 1998).

[13] **V. Martinez**, "Spool deformations. FEM analysis", CMR Prototech Report no. RP-30363-PR-01, CMR Prototech, Bergen Norway (August 2008).

[14] **P. Lunde, and K.-E. Frøysa**, "Ormen Lange ultrasonic gas flow meters. A study for establishment of corrections for pressure and temperature effects. Phase 2", CMR report, Christian Michelsen Research AS, Norway (in preparation).